Design Concepts of High-Performance Nano-Cavities

Thanh Xuan Hoang[1,*], Fangwei Wang[2], Hong-Son Chu[1], Xudong Chen[3], Christian A Nijhuis[2,4], Francisco J. García-Vidal[1,5], Png Ching Eng[1]

1. *Institute of High Performance Computing, A*STAR (Agency for Science, Technology and Research), 1 Fusionopolis Way, #16-16 Connexis North, Singapore 138632*
2. *Department of Chemistry, National University of Singapore, 3 Science Drive, Singapore 117543, Singapore*
3. *Department of Electrical and Computer Engineering, National University of Singapore, Singapore 117576, Singapore*
4. *Faculty of Science and Technology University of Twente P.O. Box 2017, Enschede 7500 AE, The Netherlands*
5. *Departamento de Física Teórica de la Materia Condensada and Condensed Matter Physics Center (IFIMAC), Universidad Autónoma de Madrid, E-28049 Madrid, Spain*

[*hoangtx@ihpc.a-star.edu.sg](mailto:hoangtx@ihpc.a-star.edu.sg)

Abstract: Based on exact analytical solutions to the Maxwell equations, we present design concepts for high-performance photonic and plasmonic nano-cavities including gap modes, Fabry-Pérot modes, collective Mie resonances, Feshbach-type BIC modes, and photonic flat bands.

1. Collective Mie Resonances

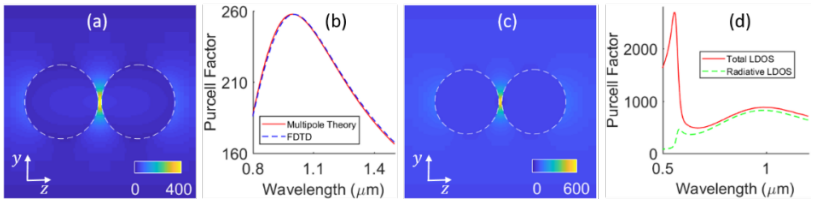

Fig. 1. (a) The imaginary component of the electric field E_z shows the gap mode confined within 10 nm between the two identical dielectric spheres, represented by the two dashed circles, with a refractive index of 3.65 and a radius of 115 nm, surrounded by air. (b) The emission rate enhancement of the z-oriented electric dipolar emitter, which is situated at the centre of the gap in (a). The peak wavelength is 1 μm. The far-field (Multipole Theory) and near-field (FDTD) approaches of calculating the Purcell factor agree excellently with each another. (c) We replace the dielectric spheres in (a) by the two identical copper spheres with a slightly smaller radius of 100 nm that ensures the collective dipole resonance to peak at the wavelength of 1 μm. (d) The total dissipation power (Total LDOS) and the corresponding radiative power (Radiative LDOS) from the dipolar emitter placed in the gap in (c).

Photonic and plasmonic concepts usually originate from atomic and molecular physics [1,2]. At the heart of these concepts is the interaction between light and material distributions. The building blocks for the material structures are usually referred to as photonic (plasmonic) atoms. Arranging these artificial atoms to form photonic (plasmonic) molecules has enabled researchers to uncover many intriguing electromagnetic analogs of molecular concepts [3,4]. For instance, Fig. 1 presents the bonding modes of the photonic and plasmonic diatomic molecules. The field hotspots associated with these bonding modes are of great interest for enhancing the interaction energy between the molecules and appropriate emitters, such as a longitudinal electric dipole (ED) placed at the centre of the gap. This interaction enhancement is known as Purcell effect in which material distributions alter the electromagnetic fluctuation of emitters' environment. The enhancement can be quantified by the Purcell factor F_P. Figure 1(b) presents the estimation of the factor associated with the longitudinal ED using far-field (Multipole Theory) and near-field (FDTD) approaches [5]. The two dielectric spheres resonate in unison and consequently form the gap mode in Fig. 1(a) with the peak wavelength at 1 μm.

Recently, plasmonic copper structures gain significant interest due to copper's plasmonic properties and its compatibility to the CMOS technology [6]. Figures 1(c) and 1(d) present the plasmonic counterpart of the gap mode in Fig. 1(a) and the associated local density of optical states (LDOS). The total LDOS comprises of absorptive and radiative components. We can estimate from Fig. 1(d) that the majority (90%) of light emission at the peak wavelength of 1 μm radiates into the far-field region. Both the near-field strength and the associated Purcell factor are on the same order as those presented in Figs. 1(a) and 1(b). In addition, the radius of the dielectric atom is only slightly larger than that of the plasmonic atom (115 nm vs 100 nm). Nevertheless, unlike the plasmonic counterpart, we will show in this presentation that dielectric atoms can form photonic molecules functioning as high-performance nano-cavities, offering high-Q and F_P factors of the order of millions. We will discuss the rich physics of collective Mie resonances [7] that elucidate the physics of photonic-crystal (PC) cavity modes, Feshbach-type BIC (bound states in the continuum) modes, and photonic flat bands. The clarity of our concept discussion comes from the Mie's exact solutions to the Maxwell equations [8,9]. In connection with the physics of collective Mie resonances, we discuss the Feshbach-type BIC mode resulting from the optimization of the well-known L3 PC defect cavity.

2. Feshbach-type BIC Mode from L3 Photonic-Crystal Defect Cavity

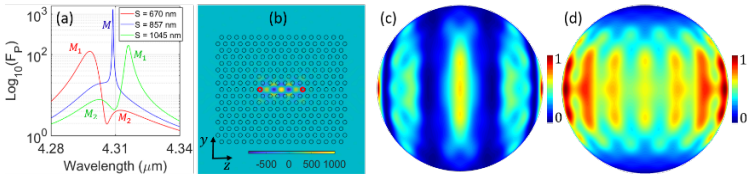

Fig. 2. Feshbach-type BIC cavity from the optimization of the L3 PC defect mode. (a) Shifting the two edge air holes, marked by the red circles in (b), results in the overlapping resonant mode, marked by M, that is known as Feshbach resonance in nuclear physics. (b) The imaginary component of the E_z field distribution of the optimal M mode. (c) The destructive interference results in fewer radiative channels in comparison with those from (d), represented by the line patterns, appearing on the yz radiation pattern. (d) The yz radiation pattern for the M_1mode indicates the highly radiative nature of the PC cavity defect mode.

Figure 2 presents our optimization result for the well-known L3 PC defect cavity for the technology of silicon photonics, designed for mid-infrared frequency applications [5]. The radius and period of the air holes are 353 nm and 1340 nm, respectively. The thickness of the silicon wafer is 500 nm. Figure 2(a) shows that the two M_1 and M_2 modes overlap at the shift of $S = 857$ nm to result in the Feshbach-type BIC mode that explains the dramatic increase of the Purcell factor. Figures 2(b) and 2(c) show the near-field and far-field distributions associated with the optimal M mode. The radiation pattern in Fig. 2(d) corresponds to the resonant M_1 mode. The destructive interference from the overlapping resonances accounts for the light-trapping efficacy of the optimal structure that manifests itself in the fewer line features in Fig. 2(c) in comparison with those in Fig. 2(d).

3. Hybridization of Nano-antenna and Fabry-Pérot Nano-cavity

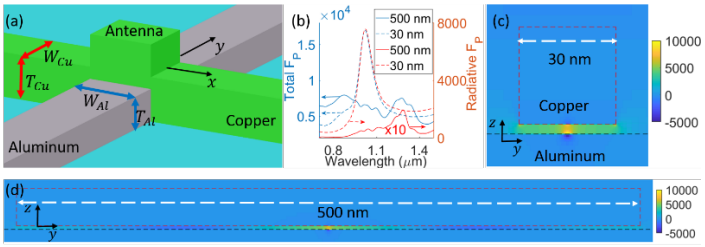

Fig. 3. (a) Schematic of an electron quantum tunneling junction (TJ). (b) The dependence of the antenna and cavity effect on the geometrical parameters of the TJ. (c)-(d) The electric field distributions of the Fabry-Pérot modes supported by the two TJs.

Figure 3(a) shows a schematic of an electron tunneling junction (TJ) formed by an insulator layer sandwiched between the Al and Cu electrodes which also serve as plasmonic waveguides. We are interested in these structures due to its geometrical simplicity as well as its potential in offering ultra-small physical footprints for light and plasmonic devices [6]. Figure 3(b) shows the effect of reducing the widths of the Al and Cu waveguides in which we fix the thicknesses to be $T_{Al} = 20$ nm and $T_{Cu} = 30$ nm. For the large TJ with $W_{Al} = W_{Cu} = 500$ nm, the outcoupling light is orders of magnitude lower than the optimal structure with $W_{Al} = W_{Cu} = 30$ nm. For the optimal structure, we have optimized the geometrical parameters so that the lowest-order Fabry-Pérot mode of the 3-nm gap overlaps spectrally with the antenna mode supported by the miniature TJ. Figures 3(c) and 3(d) show the electric field distributions of the Fabry-Pérot modes supported by the 30-nm and 500-nm TJs, respectively. The propagation lengths of the strongly confined modes are few tens of nm which explains the superior performance of the small TJ. Experimentally, we will present substantial enhancements of light emission efficiency from miniature TJs.

Acknowledgement

This research is supported by A*STAR under its Career Development Fund (C210112012).

References

[1] M. Bayer, et al., "Optical Modes in Photonic Molecules," Phys. Rev. Lett. **81** 2582-2585 (1998).
[2] E. Prodan, et al., "A Hybridization Model for the Plasmon Response of Complex Nanostructures," Science **302** 419-422 (2003).
[3] T. X. Hoang, et al., "Fano resonances from coupled whispering–gallery modes in photonic molecules," Opt. Express **25** 13125-13144 (2017).
[4] K. Liao, et al., "Photonic molecule quantum optics," Adv. Opt. Photonics **12** 60-134 (2020).
[5] T. X. Hoang, et al., "High-Performance Dielectric Nano-cavities for Near- and Mid-infrared Frequency Applications," J. Opt., (2022).
[6] F Wang, et al., "Spatial Control over Stable Light-Emission from AC-Driven CMOS-Compatible Quantum Mechanical Tunnel Junctions," Laser Photonics Rev. **16** 2100419 (2022)
[7] T. X. Hoang, et al., "Collective Mie Resonances for Directional On-Chip Nanolasers," Nano Lett. **20** 5655-5661 (2020).
[8] T. X. Hoang, et al., "Interpretation of the scattering mechanism for particles in a focused beam," Phys. Rev. A **86** 033817 (2012).
[9] T. X. Hoang, et al., "Focusing and imaging in microsphere-based microscopy," Opt. Express **23** 12337-12353 (2015).